

Article

# Performance of a Ni-Cu-Co/Al<sub>2</sub>O<sub>3</sub> Catalyst on In-Situ Hydrodeoxygenation of Bio-derived Phenol

Huiyuan Xue <sup>1,2</sup>, Jingjing Xu <sup>1,2</sup>, Xingxing Gong <sup>1,2</sup> and Rongrong Hu <sup>1,2,\*</sup> <sup>1</sup> Key Laboratory of Applied Surface and Colloid Chemistry, Ministry of Education, Xi'an 710062, China; xuehy@snnu.edu.cn (H.X.); XXGong0712@163.com (X.G.); xjj315@snnu.edu.cn (J.X.)<sup>2</sup> School of Chemistry and Chemical Engineering, Shaanxi Normal University, Xi'an 710062, China

\* Correspondence: rrhu@snnu.edu.cn; Tel.: +86-29-81530726

Received: 16 October 2019; Accepted: 9 November 2019; Published: 14 November 2019



**Abstract:** The in-situ hydrodeoxygenation of bio-derived phenol is an attractive routine for upgrading bio-oils. Herein, an active trimetallic Ni-Cu-Co/Al<sub>2</sub>O<sub>3</sub> catalyst was prepared and applied in the in-situ hydrodeoxygenation of bio-derived phenol. Comparison with the monometallic Ni/Al<sub>2</sub>O<sub>3</sub> catalyst and the bimetallic Ni-Co/Al<sub>2</sub>O<sub>3</sub> and Ni-Cu/Al<sub>2</sub>O<sub>3</sub> catalysts, the Ni-Cu-Co/Al<sub>2</sub>O<sub>3</sub> catalyst exhibited the highest catalytic activity because of the formation of Ni-Cu-Co alloy on the catalyst characterized by using X-ray powder diffraction (XRD), temperature programmed reduction (TPR), N<sub>2</sub> physisorption, scanning electron microscope (SEM), and transmission electron microscope (TEM). The phenol conversion of 100% and the cyclohexane yield of 98.3% could be achieved in the in-situ hydrodeoxygenation of phenol at 240 °C and 4 MPa N<sub>2</sub> for 6 h. The synergistic effects of Ni with Cu and Co of the trimetallic Ni-Cu-Co/Al<sub>2</sub>O<sub>3</sub> catalyst played a significant role in the in-situ hydrodeoxygenation process of phenol, which not only had a positive effect on the production of hydrogen but also owned an excellent hydrogenolysis activity to accelerate the conversion of cyclohexanol to cyclohexane. Furthermore, the catalyst also exhibited excellent recyclability and good potential for the upgrading of bio-oils.

**Keywords:** bio-derived phenol; Ni-Cu-Co/Al<sub>2</sub>O<sub>3</sub>; in-situ hydrodeoxygenation; cyclohexane; hydrogenolysis

## 1. Introduction

Biomass is one of the most abundant renewable resources on the earth. Bio-oil, produced from biomass, is recognized as a green feedstock for the production of chemicals and fuels [1,2]. Bio-oil has the advantages of a higher energy density than the original biomass, secure storage and transportation, and flexible use. However, the much higher oxygen content in bio-oils results in lower heating value and poorer stability compared to crude oil, which makes it difficult to use directly as engine fuels or even oil additives without further upgrading [3,4]. Therefore, the study of upgrading bio-oils has attracted much attention in recent years due to environmental and sustainable concerns. One of the promising routines to upgrading bio-oils is catalytic hydrodeoxygenation (HDO) [4,5]. However, the conventional HDO process needs excessive hydrogen to maintain high hydrogen pressure of 7–20 MPa [6,7], which inevitably increases the storage and transportation costs and safety risks of hydrogen. Although the HDO process is useful, it is unfavorable for the production of fuels [8–10] and estimated to need approximately 0.11 kg H<sub>2</sub>/L oil [9] by a techno-economic analyses. Therefore, reducing external hydrogen supply, such as using in-situ generated hydrogen, might be one of the augmented approaches for improving the economic feasibility [11]. More importantly, compared with the conventional HDO process, the in-situ hydrodeoxygenation (in-situ HDO) process is more flexible without the complicated equipment and suited for the distributed upgrading of bio-oils [12], which helps to expand its industrial application.

In recent years, the in-situ HDO has become a trend in the bio-oil upgrading research [12–15]. Fisk et al. [12] reported that the Pt/Al<sub>2</sub>O<sub>3</sub> catalyst had high activity for the in-situ HDO of a model bio-oil, and after upgrading the oxygen content of the model oil decreased from 41.4 wt% to 2.8 wt%. Other noble metal catalysts such as Pd/AC [13], Ru/MCM-41 [16] and Pd/C [11] also showed high activity for the in-situ HDO of some model components in bio-oils. Feng et al. [17] reported that the in-situ HDO process could not only reduce the usage of external hydrogen but also significantly improve the yield of target products in the bio-oil upgrading. Xiang et al. [18] used Raney Ni and a Pd/Al<sub>2</sub>O<sub>3</sub> catalyst in the in-situ hydrogenation of phenol, o-cresol, and p-tert-butylphenol. They found that the activity of the in-situ generated hydrogen from aqueous-phase reforming (APR) was different from that of H<sub>2</sub> gas used in the hydrogenation of bio-oil. For example, the hydrogen generated from APR favored the production of cyclohexanone, while the hydrogen from H<sub>2</sub> gas favored the generation of cyclohexanol in the hydrogenation reaction of phenol.

Ni-based catalysts also showed excellent catalytic activity for the upgrading of bio-oils [14,19–21]. Putra et al. [14] reported phenol conversion could increase to 86.75% when in-situ glycerol aqueous reforming and phenol hydrogenation over Raney Ni catalyst. Xu et al. [19] used Raney Ni for the in-situ HDO of phenol and found more than 64% phenol could be converted to cyclohexanol at 220 °C. However, they had low selectivity for some oxygen-free products. The combination with acidic sites could help to increase its deoxygenation ratio of bio-oil. Wang et al. [22] found the total deoxygenation ratio of bio-oil could reach 99.6% over the ZrNi/Ir-ZSM-5 and Pd/C catalysts through in-situ HDO by using methanol as a liquid hydrogen donor. When using Raney Ni and Nafion/SiO<sub>2</sub> catalysts in the in-situ hydrodeoxygenation of bio-derived phenol, the phenol conversion and the total yield of cyclohexane can reach respectively 100% and 87%, respectively [23]. Feng et al. [15] reported that the catalysts of Raney Ni and HZSM-5 also yielded 70–90% cyclohexanes and hydrocarbons in the in-situ hydrodeoxygenation of biomass-derived phenolic compounds. Besides, the production of hydrogen obtained from aqueous-phase reforming of liquid hydrogen donors also had a significant effect on the in-situ HDO of bio-oils. Zeng et al. [16] observed that although methanol, ethanol, formic acid, and acetic acid could generate hydrogen, the product distributions of bio-oils after upgrading were very different due to their different productivity of hydrogen. Hence, another important strategy is to improve the productivity of hydrogen in the in-situ HDO of bio-oils. Many researchers have focused on the effect of liquid hydrogen donors [11,16,18] or the ratio of the hydrogen donors to phenols [13,14,22–24] on the hydrogen availability. Unfortunately, few works have reported the effect of the multifunctional catalysts on hydrogen production in this process. Raney Ni [14] and the monometallic Ni catalyst [24] have an excellent hydrogen yield for the oxygenates aqueous-phase reforming. However, a considerable amount of work [25–30] has demonstrated that the bimetallic or trimetallic catalysts have positive effects on hydrogen production in the oxygenates reforming and inhibit the sintering of the active phase due to their excellent dispersion and electronic properties. Also, bimetallic catalysts such as Ni-Cu/Al<sub>2</sub>O<sub>3</sub> [31], Ni-Fe/Al<sub>2</sub>O<sub>3</sub> [32,33], Ni-Fe/MCSs [34], and Ni-Co/HZSM-5 [35] had excellent catalytic activity for converting bio-derived phenols into hydrocarbons by the conventional HDO with external hydrogen gas. Recently, Zhang et al. [36] prepared the Cu-Ni/ZrO<sub>2</sub> catalysts for in-situ HDO of oleic acid to heptadecane and found the bimetallic catalysts had higher activities compared with the monometallic Ni catalysts because of the synergistic effect between Ni and Cu alloy. These results indicated that the use of the bimetallic or trimetallic catalysts could improve both the hydrogen availability and the deoxygenation ratio of bio-oil in the in-situ HDO process.

In this study, a trimetallic Ni-Cu-Co/Al<sub>2</sub>O<sub>3</sub> catalyst was prepared and applied in the in-situ hydrodeoxygenation of phenol. Phenol derivatives comprise up 30 wt% of bio-oil [37], and therefore, phenol is suitable as a probe molecular to understand the primary pathways of in-situ HDO reaction. The various reaction conditions such as temperature, N<sub>2</sub> pressure, reaction time, the molar ratio of water/methanol, and liquid hydrogen donors on the in-situ HDO reaction were studied. The recyclability of the Ni-Cu-Co/Al<sub>2</sub>O<sub>3</sub> catalyst was also tested. Furthermore, the relationships of the structure and catalytic activity of the Ni-Cu-Co/Al<sub>2</sub>O<sub>3</sub> catalyst were studied by X-ray powder diffraction

(XRD), BET analysis, temperature programmed reduction (TPR), scanning electron microscope (SEM), and transmission electron microscope (TEM), and the synergistic effects of Ni with Co and Cu on the in-situ hydrodeoxygenation of phenol was discovered.

## 2. Results and Discussion

### 2.1. Structural Characterization

The XRD pattern of the fresh catalysts is presented in Figure 1. A nickel phase at  $2\theta = 44.5$ , 51.8 and  $76.4^\circ$  (JCPDS #04-0850), and a copper phase at  $2\theta = 43.4$ , 50.6 and  $74.3^\circ$  (JCPDS #65-9743) were observed in 20Ni/Al and 5Cu/Al, respectively. The 5Co/Al catalyst showed a very tiny diffraction peak attributed to Co, indicating that the Co species were highly dispersed on the surface of the  $\text{Al}_2\text{O}_3$  support. In Figure 1, it is noted that the prepared 20Ni-5Co/Al catalyst exhibits a diffraction peak similar to that of the fresh 20Ni/Al at around  $2\theta = 44.4$ . However, detailed studies of the diffraction peaks of the sample showed that it shifted towards a higher angle, indicating that a bimetallic alloy was formed due to the incorporation of cobalt, which was different from the diffraction peaks of the physically mixed metal samples [38]. Besides, in the 20Ni-5Cu-5Co/Al sample, the slight shift of the diffraction peak of Ni-Cu-Co at 44.26 (111) was also noticeable, indicating the formation of trimetallic alloy nanoparticles. A similar observation was also made by Singh et al. [39]. The diffraction peak at  $44.26^\circ$  corresponding to a nickel fcc phase was attributed to the Ni-Cu-Co solid solution caused by the incorporation of cobalt and copper [40,41].

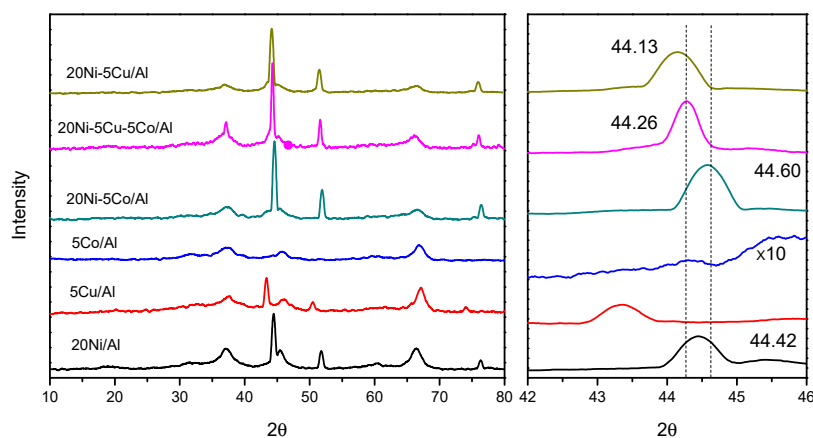
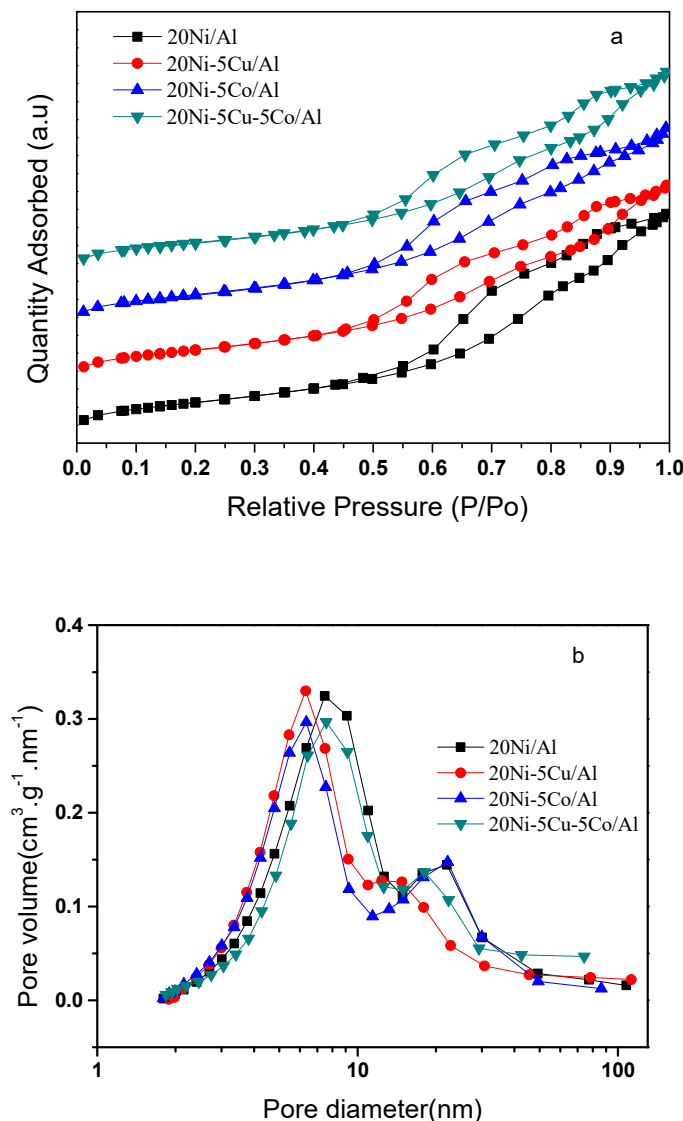


**Figure 1.** X-ray powder diffraction (XRD) patterns of the fresh catalysts.

The textural properties of the fresh catalysts are summarized in Table 1. The surface area of the  $\text{Al}_2\text{O}_3$  support was  $221 \text{ m}^2/\text{g}$ . After the incorporation of metal, the impregnated catalysts owned a lower surface area due to pore blockage during metal deposition.  $\text{N}_2$  adsorption-desorption isotherms and pore size distributions are conducted to determine the structure of the samples, which is presented in Figure 2. All the isotherms obtained for these catalysts exhibit a type IV isotherm shape. The BJH pore size distribution (Figure 2b) indicates that the majority of pores were mesopores with pore sizes smaller than 10 nm.

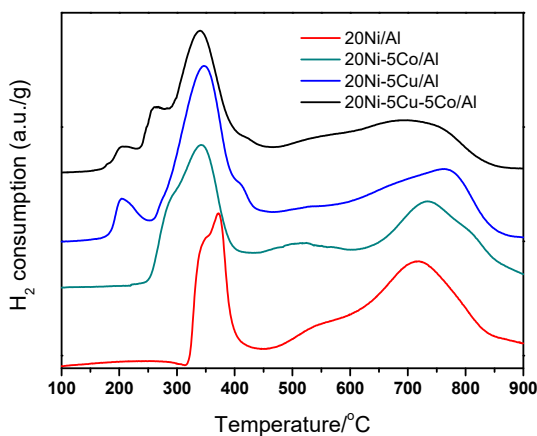
**Table 1.** The textural properties of the fresh catalysts.

Catalyst	Surface Area		Pore Volume	Pore Size
	$\text{m}^2/\text{g}$	$\text{cm}^3/\text{g}$		
$\text{Al}_2\text{O}_3$	221	0.33	9.96	
20Ni/Al	82	0.20	9.54	
20Ni-5Cu/Al	80	0.18	8.71	
20Ni-5Co/Al	82	0.18	8.63	
20Ni-5Cu-5Co/Al	78	0.18	9.19	



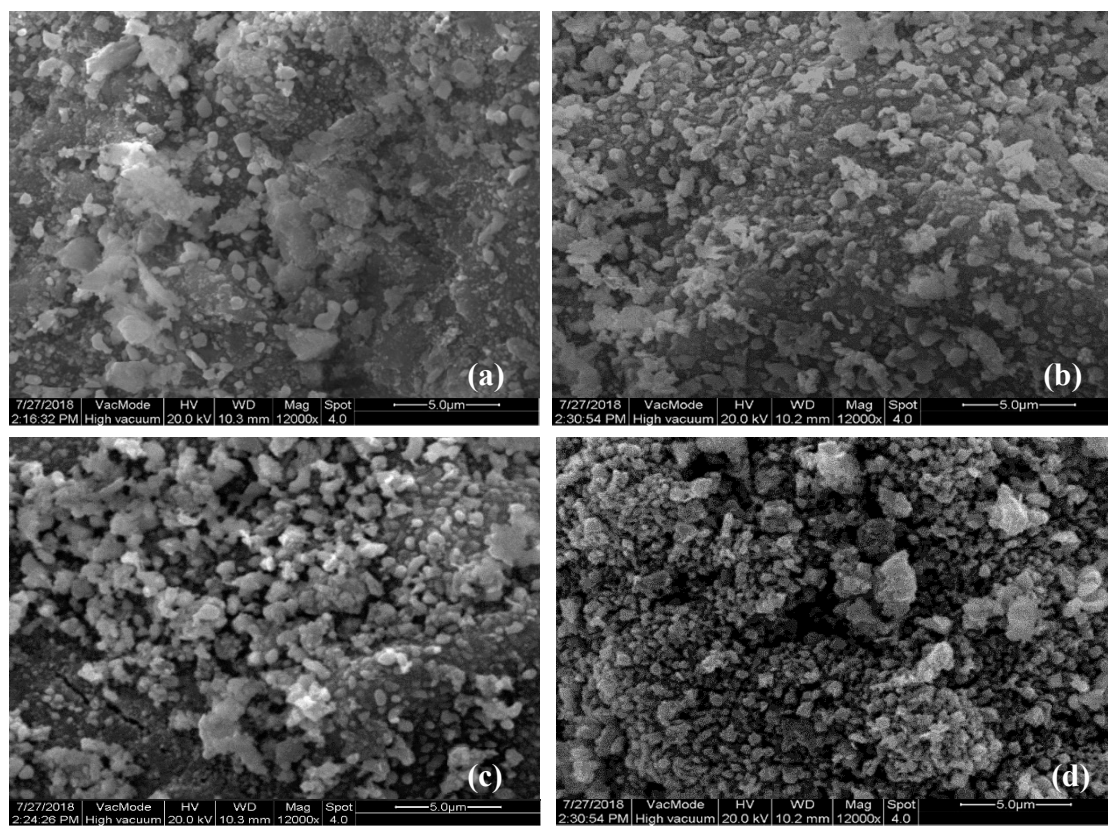
**Figure 2.** (a)  $\text{N}_2$  adsorption-desorption isotherms and (b) pore size distribution calculated from the BJH desorption branch.

Figure 3 shows the TPR results of the fresh samples. The 20Ni/Al catalyst clearly showed multi broad peaks at 350 °C, 550 °C, and 700 °C. The first peak was associated with the reduction of  $\text{Ni}^{2+}$  to  $\text{Ni}^0$ , showing a weak interaction between  $\text{NiO}$  and  $\text{Al}_2\text{O}_3$  support [29]. The other two peaks were broader reduction peaks from 480 °C to 800 °C. The wideness of the peaks suggested a stronger interaction between  $\text{NiO}$  and  $\text{Al}_2\text{O}_3$ . As reported by Shi et al. [42], there were octahedrally and tetrahedrally coordinated  $\text{Ni}^{2+}$  in the Ni supported catalysts, and the high temperature peak at 700 °C corresponded to the reduction of tetrahedrally coordinated  $\text{Ni}^{2+}$  since it was less reducible than the former. The 20Ni-5Co/Al catalyst clearly showed three distinct peaks. The reduction of  $\text{Ni}^{2+}$  to  $\text{Ni}^0$  and  $\text{Co}^{3+}$  to  $\text{Co}^{2+}$  were responsible for the peaks at 300–410 °C, and the second weak peak at 500 °C corresponded to the complete reduction of cobalt [30]. For 20Ni-5Cu-5Co/Al, the area of the peak related to the reduction of tetrahedrally coordinated  $\text{Ni}^{2+}$  decreased, indicating that, for this sample, the amount of  $\text{NiAl}_2\text{O}_4$  species was decreased [42]. The TPR results implied that the addition of cobalt and copper improved the reducibility of  $\text{NiO}$ , and hence more metallic Ni could be exposed in the trimetallic 20Ni-5Cu-5Co/Al catalyst.



**Figure 3.** Spectra of the fresh catalysts.

The SEM images of the fresh samples are presented in Figure 4 and they displayed similar morphologies, i.e., rough surfaces and small grains. When compared with the 20Ni/Al catalysts, the bimetallic and trimetallic catalysts showed smaller particle sizes, which showed that the addition of Co or Cu could restrain agglomeration and promote the dispersion of the nickel species on the  $\text{Al}_2\text{O}_3$  support surface.



**Figure 4.** Scanning electron microscope (SEM) images of the fresh catalysts. 20Ni/Al (a), 20Ni-5Cu/Al (b), 20Ni-5Co/Al (c), 20Ni-5Cu-5Co/Al (d).

The TEM images and the particle size distribution for the fresh catalysts are presented in Figure 5. The particle distribution of the 20Ni/Al catalyst was 20–40 nm. When adding Co and Cu in 20Ni/Al, the particle distribution results indicated that it had a higher portion of smaller size in the 20Ni-5Cu-5Co/Al catalyst, which was attributed to the geometric and stabilizing effect of these metals [43]. The addition

of cobalt or copper may show a “dilution effect” [44] or act as an inert spacer [45] on the surface of Ni species, forming much smaller metal alloy particles. The microstructure of 20Ni-5Cu-5Co/Al was also characterized by high-resolution transmission electron microscopy (HRTEM) and the crystalline fringe was measured to be 0.205 nm, which corresponds to the (111) interplanar spacing of the fcc structure of Ni-Cu-Co [46]. These images further confirmed the formation of the Ni-Cu-Co alloy, which was consistent with the XRD results.

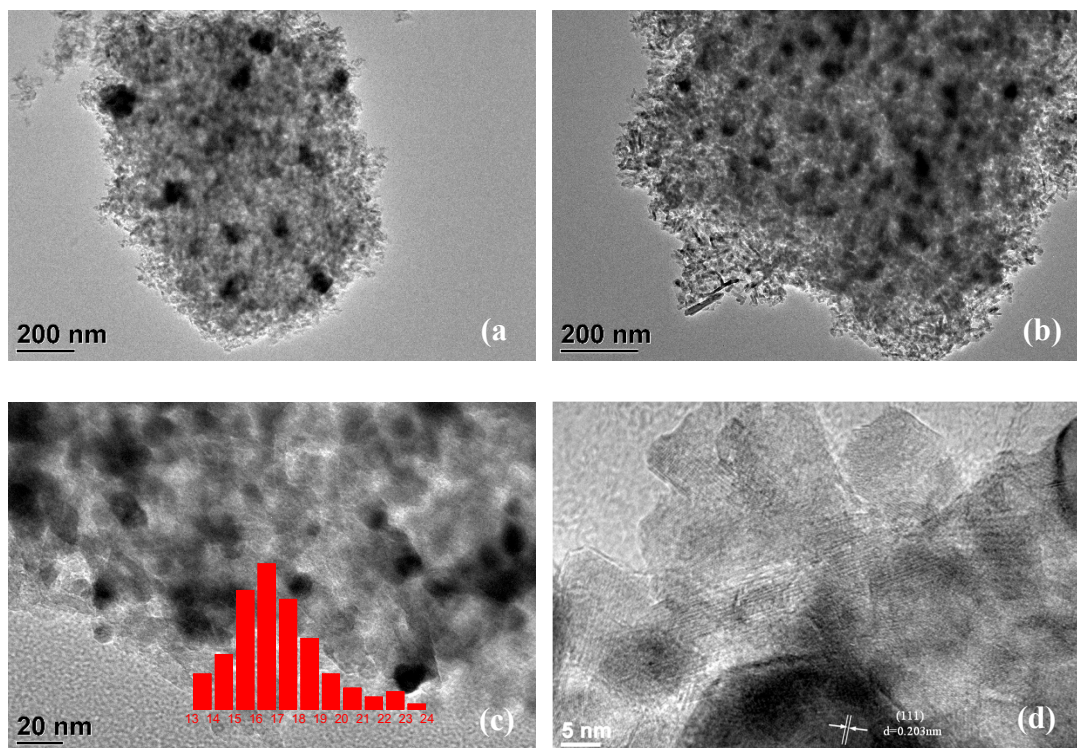


**Figure 5.** Images of the fresh catalysts. 20Ni/Al (**a**), 20Ni-5Cu-5Co/Al (**b-d**).

## 2.2. Performance of Ni-Based Catalysts in the *in-situ* Hydrodeoxygenation (HDO) of Phenol

According to the previous studies, the *in-situ* HDO process of phenol includes two main reactions: Hydrogen generation from the aqueous-phase reforming (APR) of methanol, and hydrodeoxygenation of phenol. Ni-based catalysts had been reported of excellent activities in both methanol aqueous-phase reforming and hydrodeoxygenation of phenols.

### 2.2.1. Hydrogen Production from Methanol Aqueous-Phase Reforming over Ni-Based Catalysts

The hydrogen used in the *in-situ* HDO, obtained from methanol aqueous-phase reforming, had an important effect on the HDO of phenol. For the over-all methanol aqueous-phase reforming, the hydrogen production is always accompanied by several side reactions, such as methanol decomposition, water gas shift reaction, methanation, and F-T reactions [29]. Therefore, the hydrogen yield is highly related to the performance of the catalysts. In order to further improve the catalytic activity and product selectivity, the second metal such as Co or Cu was often used to add into the Ni-based catalysts to tune surface active Ni by changing metal particle sizes or strengthen metal-support interaction. They could help to enhance water gas shift reaction or inhibit methanation reaction for higher hydrogen yield in the reforming reactions [26,27,29,30]. Table 2 shows the conversion and yield of gas products during the APR of methanol over the different Ni-based catalysts. From it, for all these catalysts, only  $H_2$ ,  $CO_2$ ,  $CO$ , and  $CH_4$  could be detected in significant concentrations in the gas products. For the 20Ni/Al catalyst, the hydrogen yield was about 1.05 mol/mol  $CH_3OH$  and the water/methanol consumption was only 0.37, indicating that the methanol APR was part of the reaction. Besides, the amount of  $CO$  formed over

this catalyst was more than CO<sub>2</sub>, which confirmed that it was favorable for the decomposition reaction of methanol rather than the APR reaction itself and the decomposition reaction on Ni species was in charge of generating more CO. After adding a small amount of Co or Cu into the 20Ni/Al catalyst, the hydrogen yield rapidly increased to 1.31 and 1.75 mol/mol CH<sub>3</sub>OH, respectively. It was also observed that with the 20Ni-5Cu/Al and 20Ni-5Co/Al catalyst, the water/methanol consumption increased and the amounts of CO decreased, which implied both Cu and Co could promote the methanol reforming and water gas shift reaction and produce more H<sub>2</sub> and CO<sub>2</sub>. Notably, CH<sub>4</sub> due to CO or/and CO<sub>2</sub> hydrogenation over the 20Ni/Al catalyst in the reforming was not observed in the 20Ni-5Cu/Al and 20Ni-5Co/Al catalyst, indicating that the Ni-Cu or Ni-Co alloy phase may be responsible for reducing the effects of the methanation reaction. On the 20Ni-5Cu-5Co/Al catalyst, the H<sub>2</sub> yield was 2.15 mol/mol CH<sub>3</sub>OH. Such a high amount of hydrogen showed the APR reaction and water gas shift reaction may dominate over the 20Ni-5Cu-5Co/Al catalyst, evidenced by an increase in both CO<sub>2</sub> production and water/methanol consumption. Indeed, for the 20Ni-5Cu-5Co/Al catalyst, the adding of Co and Cu in the Ni/Al catalyst affected in a positive way for the production of hydrogen due to the synergistic effects of Ni-Cu-CO alloy.

**Table 2.** The conversion and yield of gas products during the aqueous-phase reforming of methanol over the different Ni-based catalysts.

Sample	Conversion (%)		Water/Methanol Consumption	Yield (mol/mol CH <sub>3</sub> OH)			
	CH <sub>3</sub> OH	H <sub>2</sub> O		H <sub>2</sub>	CO	CH <sub>4</sub>	CO <sub>2</sub>
20Ni/Al	52	5.55	0.37	1.05	0.34	0.09	0.09
20Ni-5Co/Al	53.4	6.9	0.45	1.31	0.26		0.27
20Ni-5Cu/Al	64.1	13.5	0.74	1.75	0.17		0.47
20Ni-5Cu-5Co/Al	75.4	18.3	0.85	2.15	0.13		0.62

Reaction conditions: 30 g deionized water, 15 g methanol, and 0.5 g catalyst, 240 °C, 4 MPa N<sub>2</sub>, 6 h.

## 2.2.2. In-situ HDO of Phenol over Ni-based Catalysts

The performances of the prepared catalysts in the HDO of phenol with H<sub>2</sub> and the in-situ HDO of phenol with methanol are shown in Figure 6a,b, respectively. From Figure 6a, all of the Ni-based catalysts exhibited pretty high activity in the phenol conversion. At high initial pressure of 4 MPa H<sub>2</sub>, more than 50% phenol could yield the deep hydrogenated component of cyclohexane over these catalysts. Especially for the 20Ni-5Cu-5Co/Al catalyst, it could produce nearly 99% cyclohexane, showing its excellent activity for the conventional HDO of phenol. Interestingly, when the H<sub>2</sub> initial pressure decreased to 0.5 MPa, less than 2% cyclohexane could be yielded and benzene, cyclohexanone and cyclohexanol were the main productions. Obviously, the changes might be related to the amount of hydrogen. The low hydrogen pressure of 0.5 MPa led to a decrease of H<sub>2</sub> solubility in the liquid phase and stabilized the formation of cyclohexanone and cyclohexanol.

Figure 6b is the result of the performances of the prepared catalysts in the in-situ HDO of phenol with methanol as the liquid hydrogen donor. Among the catalysts, 20Ni-5Cu-5Co/Al was the most active and the phenol conversion was nearly 100%. In contrast, monometallic 20Ni/Al and bimetallic 20Ni-5Cu/Al and 20Ni-5Co/Al exhibited approximately the same conversions of less than 80% at the conditions of this work. Regarding product distribution, cyclohexanol and cyclohexane were the main products. Cyclohexanone was also detected in low amounts on some catalysts. It is important to highlight that no benzene was formed, which showed that the direct deoxygenation of phenol to benzene hardly occurs in the in-situ HDO process of phenol in these conditions. For the monometallic 20Ni/Al catalysts, cyclohexanol mainly formed on it and its selectivity reached 78%. However, when adding a small amount of Co or Cu into 20Ni/Al, the selectivity of cyclohexanol decreased significantly and more than 60% phenol was converted to cyclohexane. After both Cu and Co was added into 20Ni/Al, the phenol conversion and cyclohexane selectivity further increased and reached 100% and

95% on 20Ni-5Cu-5Co/Al, respectively, which means the addition of Co and Cu had an essential effect on the product distribution in the in-situ HDO of phenol. In general, there were two main pathways of the hydrogenation of phenol [16]: One is the direct deoxygenation to benzene; the other one is the consecutive hydrogenation to cyclohexanone, cyclohexanol, cyclohexene, and cyclohexane, successively. Mortensen et al. [47] and Han et al. [34] quantified the rates of these steps over Ni/ZrO<sub>2</sub> and Ni-Fe/MCSs, respectively, and found that the hydrogenation rate of cyclohexanone to cyclohexanol was much higher than the hydrogenolysis rate of cyclohexanol to cyclohexane over these Ni-based catalysts. Therefore, the high selectivity for cyclohexane might imply a high activity of the catalyst in the conversion of cyclohexanol. It is worth noting that the 20Ni-5Co/Al catalyst yielded more cyclohexane than the 20Ni-5Cu/Al catalyst, indicating Co had a higher hydrogenolysis activity.

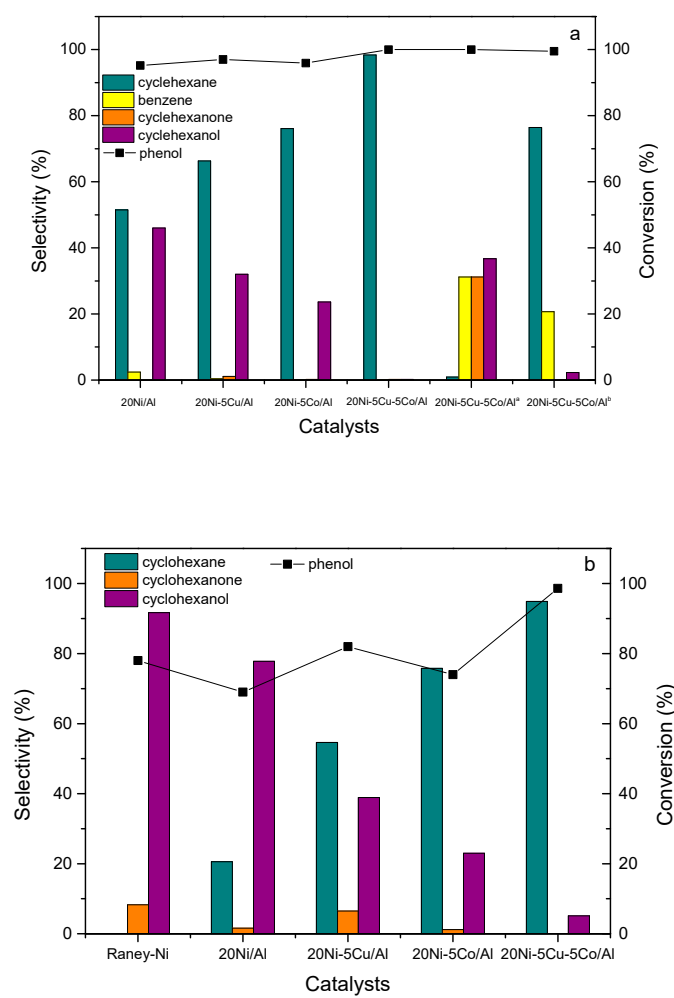


**Figure 6.** Catalytic performance of the Ni-based catalysts in the hydrodeoxygenation (HDO) of phenol with H<sub>2</sub> (a) and the in-situ HDO of phenol with methanol (b). Reaction conditions: (a) 3 g phenol and 0.5 g catalyst, 240 °C, 4 MPa H<sub>2</sub>, 6 h; (b) 30 g deionized water, 15 g methanol, 3 g phenol and 0.5 g catalyst, 240 °C, 4 MPa N<sub>2</sub>, 6 h.

To further clarify it, the hydrogenolysis of cyclohexanol to cyclohexane on the 20Ni-5Cu-5Co/Al catalyst was evaluated under 240 °C and 4 MPa H<sub>2</sub> and the results are summarized in Table 3.

**Table 3.** The hydrogenolysis of cyclohexanol over Ni-based catalysts.

Catalysts	Solvent	Conversion (%)	Selectivity (%)	
			Cyclohexene	Cyclohexane
20Ni/Al	None	72.4	—	>99.9
20Ni/Al	H <sub>2</sub> O	48.7	—	>99.9
5Cu/Al	None	23.6	—	>99.9
5Cu/Al	H <sub>2</sub> O	14.5	—	>99.9
5Co/Al	None	99.1	3.7	96.3
5Co/Al	H <sub>2</sub> O	90.2	22.6	77.4
20Ni-5Cu/Al	H <sub>2</sub> O	53.1	—	>99.9
20Ni-5Co/Al	H <sub>2</sub> O	98.7	—	>99.9
20Ni-5Cu-5Co/Al	H <sub>2</sub> O	99.3	—	>99.9

Reaction conditions: Solvent (30 g), 3 g cyclohexanol and 0.5 g catalyst, 240 °C, 4 MPa H<sub>2</sub>, 6 h.

From Table 3, the conversion of cyclohexanol over 5Co/Al was more than 90% even in water. However, it seemed the hydrogenation rate of cyclohexene over monometallic Co metal sites was slower than the dehydration rate of cyclohexanol, which led to the accumulation of cyclohexene even after 6 h. For the 5Cu/Al and 20Ni/Al catalysts, they showed much lower cyclohexanol conversion, while both of them had higher selectivity of cyclohexane. These results implied that the hydrogenation rates of cyclohexene in water over Ni and Cu metal sites were much faster than the dehydration rate of cyclohexanol. Zhao [48] had investigated the detailed kinetics of cyclohexanol dehydration and cyclohexene hydrogenation over Ni/Al<sub>2</sub>O<sub>3</sub>-HZSM-5 and they found that the hydrogenation rate of the latter showed up nearly four times higher than the dehydration rate of the former. As a consequence, only cyclohexane formed during the cyclohexanol hydrogenolysis reaction over the Ni or Cu catalysts. It must be mentioned that though Cu had a weak activity for the hydrogenolysis of cyclohexanol, once it was added to the 20Ni/Al catalyst, the yield of cyclohexane could be increased. Furthermore, when both Cu and Co were added into the 20Ni/Al catalyst, nearly 100% cyclohexane was obtained from cyclohexanol.

Therefore, the main reason for the high selectivity to cyclohexane on the 20Ni-5Cu-5Co/Al catalyst in the phenol in-situ HDO could be summarized as follows: (1) The 20Ni-5Cu-5Co/Al catalyst had a substantial effect on the amount of producing hydrogen due to the different selectivity towards methanol decomposition reaction and the water gas shift reaction. The monometallic Ni catalyst was favorable for methanol decomposition reaction and it also promoted CH<sub>4</sub> formation. The 20Ni-5Cu-5Co/Al catalyst produced more hydrogen because of its excellent activity for the water gas shift reaction. Cu and Co alloying in Ni catalyst also had a negative effect on methanation reaction compared to 20Ni/Al. Since the 20Ni-5Cu-5Co/Al catalyst had the highest amount of hydrogen among all prepared Ni-based catalysts, it could make the converted phenol yield more cyclohexane than the other catalysts. (2) The 20Ni-5Cu-5Co/Al catalyst had an excellent hydrogenolysis activity to accelerate the conversion of cyclohexanol to cyclohexane because of the synergistic effect of Ni-Cu-Co. The monometallic Co catalyst had a good activity for the hydrogenolysis of cyclohexanol. After Co was added into 20Ni-5Cu/Al catalysts, both cyclohexanol conversion and cyclohexane yield were significantly increased even in water. Therefore, the formation of Ni-Co-Cu alloy on 20Ni-5Cu-5Co/Al was responsible for its high selectivity to cyclohexane in the in-situ HDO of phenol. (3) Nickel particle size also had an essential influence on the HDO of phenol. The relatively small Ni particles were active for a high yield of cyclohexane by increasing the deoxygenation rate [49]. For the 20Ni-5Cu-5Co/Al catalyst, the formation of Cu-Co-Ni alloy showed a dilution effect on Ni species, resulted in smaller particle sizes, evidenced by XRD and TEM. As a consequent, a higher yield of cyclohexane would be achieved on this trimetallic 20Ni-5Cu-5Co/Al catalyst.

### 2.2.3. Effect of Reaction Temperature and Initial N<sub>2</sub> Pressure

The effect of temperature (120–260 °C) on the in-situ HDO of phenol at different initial N<sub>2</sub> pressure of 1–4 MPa over the 20Ni-5Cu-5Co/Al catalyst was also investigated. As displayed in Figure 7, when temperature increased from 120 °C to 260 °C, the phenol conversion increased and reached 52% and 100% at 1 and 4 MPa, respectively. At the lower temperature, it is unfavorable for the hydrogen production from methanol reforming due to an endothermic reaction, resulting in insufficient hydrogen, a lower conversion and a slower hydrogenation rate. The increase in temperature has not only an advantage to the conversion of phenol but also the selectivity of cyclohexane. When the temperature was lower than 180 °C, no cyclohexane could be detected in the products even in high initial pressure of 4 MPa. However, it showed a rapidly increasing trend with the temperature increasing from 180 °C to 260 °C, reaching 96.2% and 97.4% at 3 and 4 MPa, respectively. As mentioned previously, the formation of cyclohexane in the hydrogenation of phenol was originally from the hydrogenolysis reaction of cyclohexanol. Higher temperatures not only contributed to cyclohexanol transforming into cyclohexane [34,48] but also helped the production of more hydrogen, which could promote the hydrogenation of cyclohexene to cyclohexane. It must be mentioned that at low initial pressure, the highest selectivity of cyclohexane was less than 25% even at the high temperature, which means that the initial pressure is also one of the critical factors in the production distribution. High initial pressure increased the solubility of H<sub>2</sub> in the liquid phase, rendering more H<sub>2</sub> accessible the deep hydrogenation reaction, ultimately achieving high selectivity of cyclohexane.

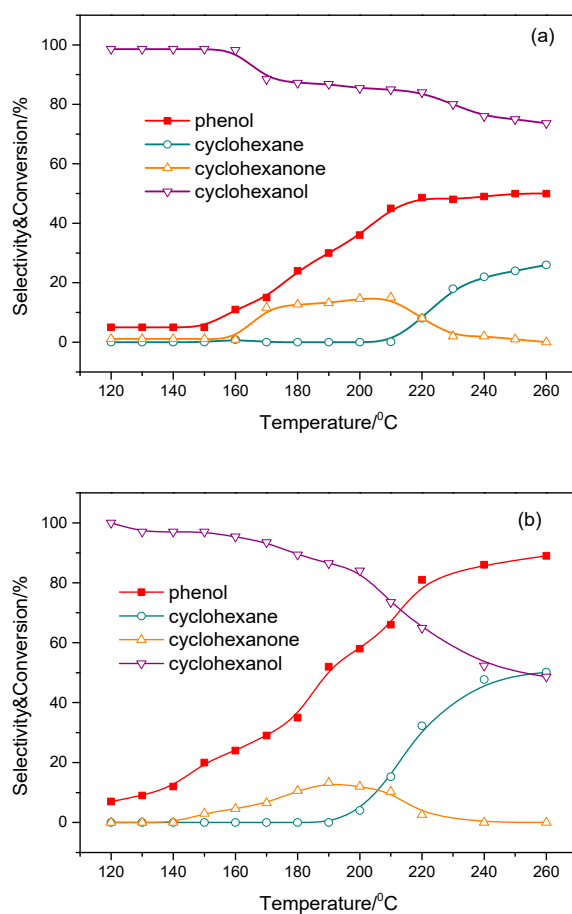


**Figure 7. Cont.**

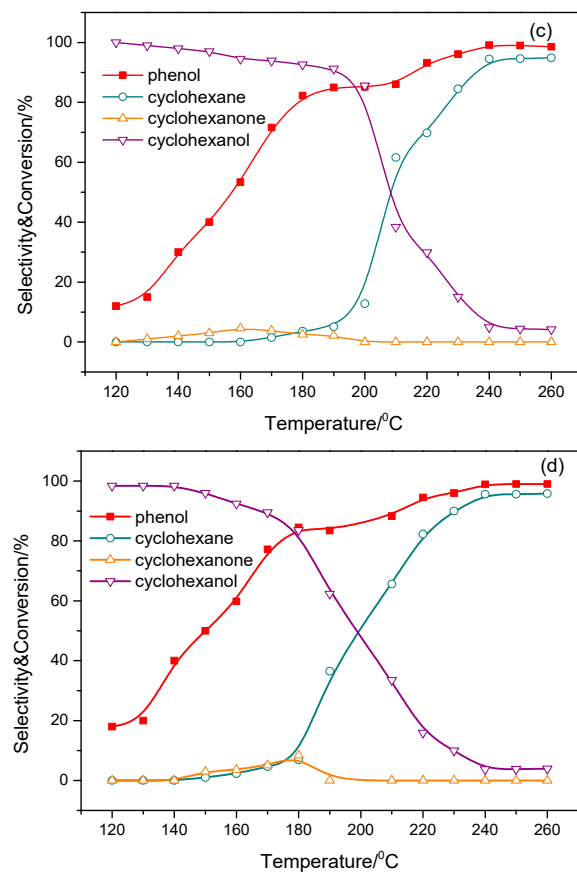


**Figure 7.** Effect of temperature on the in-situ HDO of phenol at different initial N<sub>2</sub> pressure over the 20Ni-5Cu-5Co/Al catalyst. Reaction conditions: 30 g deionized water, 15 g methanol, 3 g phenol and 0.5 g catalyst, 4 h. (a) 1 MPa initial N<sub>2</sub> pressure, (b) 2 MPa initial N<sub>2</sub> pressure, (c) 3 MPa initial N<sub>2</sub> pressure, (d) 4 MPa initial N<sub>2</sub> pressure.

#### 2.2.4. Effect of Reaction Time

The effect of the reaction time on the in-situ HDO of phenol over the 20Ni-5Cu-5Co/Al catalyst was investigated at 240 °C and 4 MPa N<sub>2</sub> over the 20Ni-5Cu-5Co/Al catalyst. From Figure 8, the conversion of phenol increased rapidly from 55.1% (1 h) to 99.2% (4 h) at the beginning and then slightly increased to 100% (5 h). Moreover, the selectivity of cyclohexane improved at the cost of the selectivity of cyclohexanol with increased reaction time. More than 95% of cyclohexane could be achieved by increasing the reaction time to 4 h. These results indicated that cyclohexanol, as an intermediate, would be converted to cyclohexane with prolonged reaction time. The hydrogenation rate of phenol to cyclohexanol might be faster than the hydrogenolysis rate of cyclohexanol to cyclohexane over the 20Ni-5Co-5Cu/Al catalyst. The hydrogenolysis of cyclohexanol was the rate-determining step of the overall reaction of phenol HDO over the catalyst with high activity for hydrogenation [34], which, as a consequence, would lead to the high selectivity of cyclohexanol in the initial phenol conversion process. After prolonging the reaction time, cyclohexane dominated the product distribution (95%) at 100% conversions, and cyclohexanol decreased to less than 5% selectivity eventually.

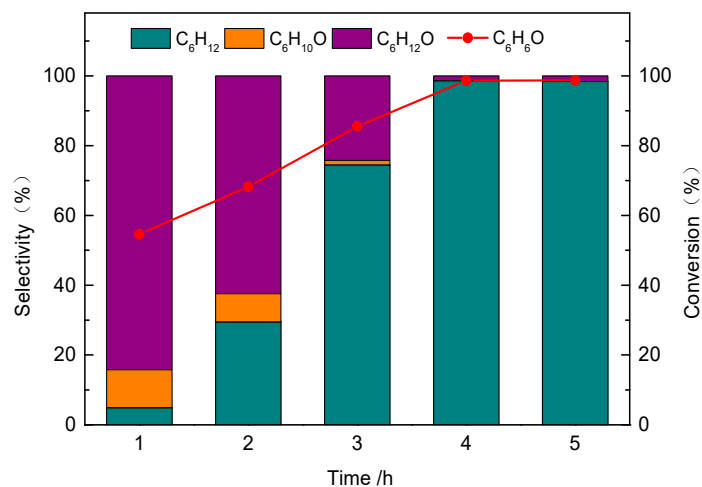


**Figure 8.** Effect of reaction time on the in-situ HDO of phenol over the 20Ni-5Cu-5Co/Al catalyst. Reaction conditions: 30 g deionized water, 15 g methanol, 3 g phenol and 0.5 g catalyst, 240 °C, 4 MPa initial N<sub>2</sub> pressure.

#### 2.2.5. Effect of the Molar Ratio of Water/Methanol

Figure 9 presents the effect of the different molar ratios of water/methanol on the in-situ HDO of phenol over the 20Ni-5Co-5Cu/Al catalyst at 240 °C and 4 MPa initial N<sub>2</sub> pressure. Since the hydrogen of the in-situ hydrogenation reaction was obtained from methanol APR, the H<sub>2</sub>O/methanol ratio had an essential effect on the hydrogenation reaction. From Figure 9, the conversion of phenol increased from 40.1% to 100%, with the increasing water/methanol ratio of 10:1 to 2.5:1. After further increasing the water/methanol ratio to 1.8:1, the conversion of phenol decreased slightly. These results showed that higher methanol concentration favored hydrogen production, thus leading to higher conversion of phenol. However, when the methanol concentration in the reactants was too high, it effectively competed for the active sites of the catalyst to block the access of reacted phenol, resulting in a decrease in phenol conversion [16,22].

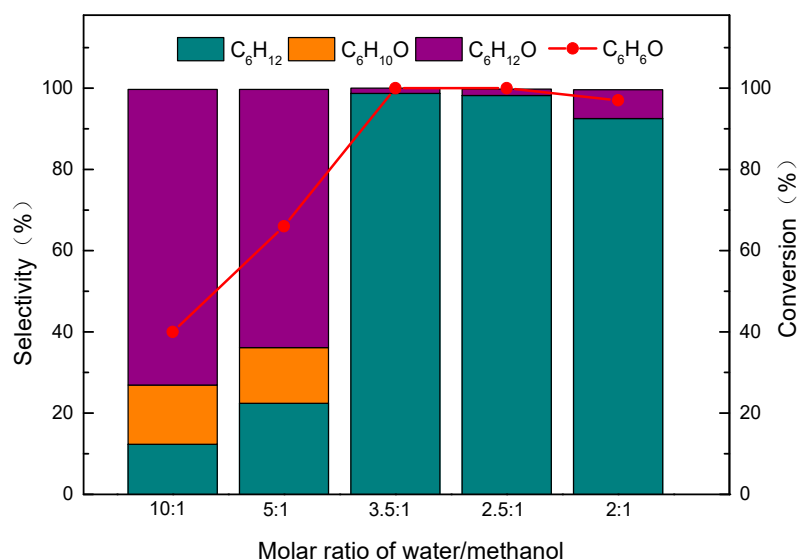


**Figure 9.** Effect of molar ratio of water/methanol on the in-situ HDO of phenol over the 20Ni-5Cu-5Co/Al catalyst. Reaction conditions: 30 g deionized water, 3 g phenol and 0.5 g catalyst, 240 °C, 4 MPa initial N<sub>2</sub> pressure, 4 h.

## 2.2.6. Effect of Liquid Hydrogen Donors

Methanol, ethanol, propanol and acetic acid were chosen as the liquid hydrogen donors and their effects on the in-situ HDO of phenol was evaluated over the 20Ni-5Co-5Cu/Al catalyst, as presented in Table 4. When ethanol was the liquid hydrogen donor, more than 90% conversion of phenol and selectivity of cyclohexane were achieved. However, when acetic acid was the liquid hydrogen donor, phenol conversion decreased to 39% under the same conditions. Meanwhile, the selectivity of cyclohexane was less than 5% and the main products of phenol in the in-situ HDO over the 20Ni-5Co-5Cu/Al catalyst were cyclohexanol and cyclohexanone. These results proved that methanol and ethanol were better than acetic acid for the in-situ HDO of phenol to cyclohexane over the 20Ni-5Co-5Cu/Al catalyst. It could be explained that the hydrogen produced by the APR of acetic acid was insufficient, and the low hydrogen pressure stabilized the formation of cyclohexanol and cyclohexanone intermediates, which was consistent with Tan et al.'s work [11]. Therefore, methanol is the best liquid hydrogen donor in the in-situ HDO process of phenol under these conditions.

**Table 4.** Effect of liquid hydrogen donors on the in-situ HDO of phenol.

Liquid Hydrogen Donors	Conversion (%)	Selectivity (%)		
		Cyclohexane	Cyclohexanone	Cyclohexanol
Methanol	100	98.6	—	1.4
Ethanol	92	93.8	—	6.2
Propanol	44	11.3	15.7	73
Acetic acid	39	2.6	21.8	75.6

Reaction conditions: 30 g deionized water, 15 g liquid hydrogen donor, 3 g phenol and 0.5 g catalyst, 240 °C, 4 MPa initial N<sub>2</sub> pressure, 4 h.

## 2.2.7. Recyclability

The recyclability of the sample is vital for practical industrial applications. The catalytic maintenance of the 20Ni-5Co-5Cu/Al catalyst was also evaluated at 240 °C, 4 MPa initial N<sub>2</sub> pressure for 4 h. After the reaction, the catalyst was then separated with the assistance of a magnet, washed with methanol several times and dried for the next cycle. Reaction results shown in Figure 10 revealed that the 20Ni-5Co-5Cu/Al catalyst could be used at least 10 times without significant decreases in catalytic conversion and selectivity, which indicated that the 20Ni-5Co-5Cu/Al catalyst exhibited excellent recyclability.

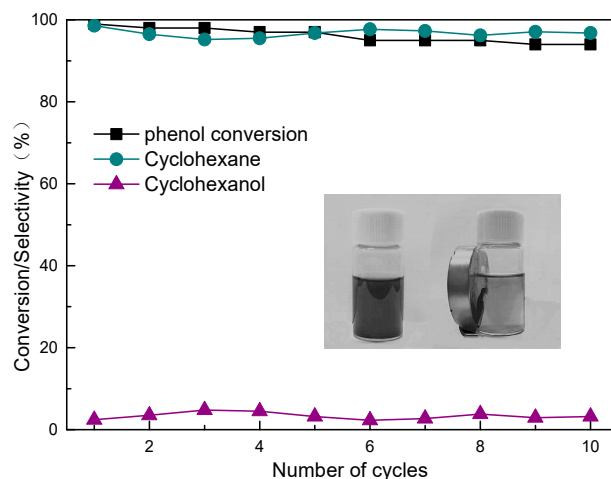


**Figure 10.** The recyclability of the 20Ni-5Co-5Cu/Al sample for in-situ HDO of phenol. Reaction conditions: 30 g deionized water, 15 g methanol, 3 g phenol and 0.5 g catalyst, 240 °C, 4 MPa initial N<sub>2</sub> pressure, 4 h.

### 3. Experimental

#### 3.1. Catalyst Synthesis

A series of Ni-based catalysts were synthesized using an impregnation method. The monometallic catalysts (20 wt% Ni/Al<sub>2</sub>O<sub>3</sub>, 5 wt% Cu/Al<sub>2</sub>O<sub>3</sub> and 5 wt% Co/Al<sub>2</sub>O<sub>3</sub>), bimetallic catalysts (20 wt% Ni-5 wt% Cu/Al<sub>2</sub>O<sub>3</sub> and 20 wt% Ni-5 wt% Co/Al<sub>2</sub>O<sub>3</sub>) and trimetallic catalyst (20 wt% Ni-5 wt% Cu-5 wt% Co/Al<sub>2</sub>O<sub>3</sub>) were prepared. Briefly, the Al<sub>2</sub>O<sub>3</sub> support was obtained through the calcination of pseudoboehmite precursor in the air at 550 °C for 4 h. The required amount of Ni(NO<sub>3</sub>)<sub>2</sub>·6H<sub>2</sub>O, Cu(NO<sub>3</sub>)<sub>2</sub>·3H<sub>2</sub>O and Co(NO<sub>3</sub>)<sub>3</sub>·6H<sub>2</sub>O, obtained from Aladdin Industrial Corporation (Shanghai, China), were dissolved in distilled water under ultrasound for 30 min. Then 5 g Al<sub>2</sub>O<sub>3</sub> support was added and mixed for 3 h using an ultrasonic mixer at 35 °C. The mixture was then dried at 100 °C for 12 h. Next, the sample was heated for calcination from 20 °C to 600 °C in a furnace at a rate of 1 °C/min, held at 600 °C for 5 h, then finally cooled to room temperature. Before the experiments, the catalyst was reduced in a 5% H<sub>2</sub>/95% N<sub>2</sub> mixed gas with a flow rate of 50 mL/min at 500 °C for 5 h. The prepared Ni-based catalysts are denoted as 20Ni/Al, 5Cu/Al, 5Co/Al, 20Ni-5Co/Al, 20Ni-5Cu/Al, and 20Ni-5Cu-5Co/Al for brevity.

#### 3.2. Catalyst Characterization

X-ray powder diffraction (XRD) patterns of these catalysts were measured by a Rigaku D/max2550VB3+/PC diffractometer (Rigaku International Corporation, Tokyo, Japan) using Cu K radiation at 40 KV and 40 mA. BET surface areas and average pore size of the catalysts were carried out by N<sub>2</sub> adsorption at 77 K with a Micrometric ASAP 2020 apparatus (Micromeritics GmbH, Aachen, Germany). Before measurements, the samples were degassed at 150 for 12 h. Temperature programmed reduction (TPR) of the samples was done in a Micromeritics AutoChem II 2920 apparatus equipped with TCD (Micromeritics GmbH, Aachen, Germany). A 50 mg sample was heated from room temperature to 800 °C in 10% H<sub>2</sub>/90%N<sub>2</sub>. Scanning electron microscope (SEM) images were recorded using an FEI Quanta 200 instrument (FEI, Eindhoven, Netherlands). High-resolution transmission electron microscopy (HRTEM) images were recorded using a JEM-2100 TEM Field Emission Electron Microscope (JEOL GmbH, Freising, Germany).

#### 3.3. Activity Tests

The experiments were performed in a 100 mL high-pressure autoclave. The typical experimental conditions are as follows: 30 g deionized water, 15 g methanol, 3 g phenol, and 0.5 g catalyst were added to the autoclave. Before the reaction, the autoclave was washed five times with 5 MPa of N<sub>2</sub> to remove air. The autoclave was then heated to 130–250 °C and kept for 1–4 h with the stirring speed of 600 rpm. After finishing the experiment, the autoclave was cooled to room temperature. All the gas and liquid products were collected and analyzed by using a gas chromatography (Jingketianmei Instrument, Shanghai, China) equipped with thermal conductivity detector (TCD) and gas chromatography equipped with flame ionization detector (FID), respectively. The conversion of reactants, the selectivity to liquid products, the yield of gas products were defined as follows:

$$\text{Conversion} = \frac{(\text{moles of reactants})_{\text{in}} - (\text{moles of reactants})_{\text{out}}}{(\text{moles of reactants})_{\text{in}}} \times 100\%$$

$$\text{Selectivity of liquid product}_i = \frac{\text{moles of product}_i}{(\text{moles of phenol})_{\text{in}} - (\text{moles of phenol})_{\text{out}}} \times 100\%$$

$$\text{Yield of gas product}_i = \frac{\text{moles of gas product}_i}{\text{moles of methanol}_{\text{in}}}$$

#### 4. Conclusions

In this study, we prepared a series of Ni-based catalysts for the in-situ HDO process of biomass-derived phenol to cyclohexane. The trimetallic 20Ni-5Co-5Cu/Al catalyst presented the highest activity compared to the other monometallic catalysts or bimetallic catalysts. The phenol conversion of 100% and the cyclohexane yield of 98.3% could be obtained in the in-situ HDO of phenol at 240 °C and 4 MPa initial N<sub>2</sub> pressure. The high catalytic activity of the 20Ni-5Co-5Cu/Al catalyst could be attributed to the formation of Ni-Cu-Co alloy, which had the strong positive synergistic effects on the generation of hydrogen from the methanol aqueous-phase reforming and hydrodeoxygenation of phenol. The catalyst also showed excellent recyclability and exhibited good potential for upgrading the bio-oil to reduce the oxygen content by the in-situ hydrodeoxygenation.

**Author Contributions:** Conceptualization, H.X.; validation, H.X., X.G. and J.X.; writing—original draft preparation, H.X.; writing—review and editing, R.H.; funding acquisition, R.H.

**Funding:** Gratitude for the support from the National Natural Science Foundation of China (21276254, 21636006) and the Fundamental Research Funds for the Central Universities (GK201603051, GK201601005).

**Conflicts of Interest:** The authors declare no conflict of interest.

#### References

- Kunkes, E.L.; Simonetti, D.A.; West, R.M.; Serrano-Ruiz, J.C.; Gartner, C.A.; Dumesic, J.A. Catalytic conversion of biomass to monofunctional hydrocarbons and targeted liquid-fuel classes. *Science* **2008**, *322*, 417–421. [[CrossRef](#)]
- Li, C.Z.; Zhao, X.C.; Wang, A.Q.; Huber, G.W.; Zhang, T. Catalytic Transformation of Lignin for the Production of Chemicals and Fuels. *Chem. Rev.* **2015**, *115*, 11559–11624. [[CrossRef](#)]
- Mortensen, P.M.; Grunwaldt, J.D.; Jensen, P.A.; Knudsen, K.G.; Jensen, A.D. A review of catalytic upgrading of bio-oil to engine fuels. *Appl. Catal. A Gen.* **2011**, *407*, 1–19. [[CrossRef](#)]
- Wang, H.M.; Male, J.; Wang, Y. Recent Advances in Hydrotreating of Pyrolysis Bio-Oil and Its Oxygen-Containing Model Compounds. *Acs Catal.* **2013**, *3*, 1047–1070. [[CrossRef](#)]
- Yoosuk, B.; Tumnantong, D.; Prasassarakich, P. Amorphous unsupported Ni-Mo sulfide prepared by one step hydrothermal method for phenol hydrodeoxygenation. *Fuel* **2012**, *91*, 246–252. [[CrossRef](#)]
- Lu, Q.; Chen, C.J.; Luc, W.; Chen, J.G.G.; Bhan, A.; Jiao, F. Ordered Mesoporous Metal Carbides with Enhanced Anisole Hydrodeoxygenation Selectivity. *Acs Catal.* **2016**, *6*, 3506–3514. [[CrossRef](#)]
- Anand, M.; Farooqui, S.A.; Kumar, R.; Joshi, R.; Kumar, R.; Sibi, M.G.; Singh, H.; Sinha, A.K. Kinetics, thermodynamics and mechanisms for hydroprocessing of renewable oils. *Appl. Catal. A Gen.* **2016**, *516*, 144–152. [[CrossRef](#)]
- Huber, G.W.; Corma, A. Synergies between bio- and oil refineries for the production of fuels from biomass. *Angew. Chem. Int. Ed.* **2007**, *46*, 7184–7201. [[CrossRef](#)]
- Singh, N.R.; Delgass, W.N.; Ribeiro, F.H.; Agrawal, R. Estimation of Liquid Fuel Yields from Biomass. *Environ. Sci. Technol.* **2010**, *44*, 5298–5305. [[CrossRef](#)]
- Venderbosch, R.H.; Ardiyanti, A.R.; Wildschut, J.; Oasmaa, A.; Heeres, H.J. Stabilization of biomass-derived pyrolysis oils. *J. Chem. Technol. Biot.* **2010**, *85*, 674–686. [[CrossRef](#)]
- Tan, Z.; Xu, X.; Liu, Y.; Zhang, C.; Zhai, Y.; Li, Y.; Zhang, R. Upgrading Bio-Oil Model Compounds Phenol and Furfural with In Situ Generated Hydrogen. *Environ. Prog. Sustain.* **2014**, *33*, 751–755. [[CrossRef](#)]
- Fisk, C.A.; Morgan, T.; Ji, Y.Y.; Crocker, M.; Crofcheck, C.; Lewis, S.A. Bio-oil upgrading over platinum catalysts using in situ generated hydrogen. *Appl. Catal. A Gen.* **2009**, *358*, 150–156. [[CrossRef](#)]
- Zhang, D.M.; Ye, F.Y.; Xue, T.; Guan, Y.J.; Wang, Y.M. Transfer hydrogenation of phenol on supported Pd catalysts using formic acid as an alternative hydrogen source. *Catal. Today* **2014**, *234*, 133–138. [[CrossRef](#)]
- Putra, R.D.D.; Trajano, H.L.; Liu, S.D.; Lee, H.; Smith, K.; Kim, C.S. In-situ glycerol aqueous phase reforming and phenol hydrogenation over Raney Ni (R). *Chem. Eng. J.* **2018**, *350*, 181–191. [[CrossRef](#)]
- Feng, J.F.; Hse, C.Y.; Yang, Z.Z.; Wang, K.; Jiang, J.C.; Xu, J.M. Liquid phase in situ hydrodeoxygenation of biomass-derived phenolic compounds to hydrocarbons over bifunctional catalysts. *Appl. Catal. A Gen.* **2017**, *542*, 163–173. [[CrossRef](#)]

16. Zeng, Y.; Wang, Z.; Lin, W.G.; Song, W.L. In situ hydrodeoxygenation of phenol with liquid hydrogen donor over three supported noble-metal catalysts. *Chem. Eng. J.* **2017**, *320*, 55–62. [[CrossRef](#)]
17. Feng, J.; Yang, Z.; Hse, C.Y.; Su, Q.; Wang, K.; Jiang, J.; Xu, J. In situ catalytic hydrogenation of model compounds and biomass-derived phenolic compounds for bio-oil upgrading. *Renew. Energy* **2017**, *105*, 140–148. [[CrossRef](#)]
18. Xiang, Y.Z.; Li, X.N.; Lu, C.S.; Ma, L.; Yuan, J.F.; Feng, F. Reaction Performance of Hydrogen from Aqueous-Phase Reforming of Methanol or Ethanol in Hydrogenation of Phenol. *Ind. Eng. Chem. Res.* **2011**, *50*, 3139–3144. [[CrossRef](#)]
19. Xu, Y.; Long, J.; Liu, Q.; Li, Y.; Wang, C.; Zhang, Q.; Wei, L.; Xinghua, Z.; Songbai, Q.; Tiejun, W. In situ hydrogenation of model compounds and raw bio-oil over Raney Ni catalyst. *Energy Convers. Manag.* **2015**, *89*, 188–196. [[CrossRef](#)]
20. Xu, Y.; Qiu, S.; Long, J.; Wang, C.; Chang, J.; Tan, J.; Liu, Q.; Ma, L.; Wang, T.; Zhang, Q. In situ hydrogenation of furfural with additives over a RANEY (R) Ni catalyst. *Rsc Adv.* **2015**, *5*, 91190–91195. [[CrossRef](#)]
21. Huang, Y.H.; Xia, S.Q.; Ma, P.S. Effect of zeolite solid acids on the in situ hydrogenation of bio-derived phenol. *Catal. Commun.* **2017**, *89*, 111–116. [[CrossRef](#)]
22. Wang, L.; Liu, Q.; Jing, C.Y.; Mominou, N.; Li, S.Z.; Wang, H.W. In-situ hydrodeoxygenation of a mixture of oxygenated compounds with hydrogen donor over ZrNi/Ir-ZSM-5+Pd/C. *J. Alloy Compd.* **2018**, *753*, 664–672. [[CrossRef](#)]
23. Wang, L.; Ye, P.J.; Yuan, F.; Li, S.Z.; Ye, Z.X. Liquid phase in-situ hydrodeoxygenation of bio-derived phenol over Raney Ni and Nafion/SiO<sub>2</sub>. *Int. J. Hydrol. Energy* **2015**, *40*, 14790–14797. [[CrossRef](#)]
24. Xu, Y.; Li, Y.; Wang, C.; Wang, C.; Ma, L.; Wang, T.; Zhang, X.; Zhang, Q. In-situ hydrogenation of model compounds and raw bio-oil over Ni/CMK-3 catalyst. *Fuel Process. Technol.* **2017**, *161*, 226–231. [[CrossRef](#)]
25. Carrero, A.; Calles, J.A.; Vizcaino, A.J. Hydrogen production by ethanol steam reforming over Cu-Ni/SBA-15 supported catalysts prepared by direct synthesis and impregnation. *Appl. Catal. A Gen.* **2007**, *327*, 82–94. [[CrossRef](#)]
26. Liao, P.H.; Yang, H.M. Preparation of catalyst Ni-Cu/CNTs by chemical reduction with formaldehyde for steam reforming of methanol. *Catal. Lett.* **2008**, *121*, 274–282. [[CrossRef](#)]
27. Khzouz, M.; Wood, J.; Pollet, B.; Bujalski, W. Characterization and activity test of commercial Ni/Al<sub>2</sub>O<sub>3</sub>, Cu/ZnO/Al<sub>2</sub>O<sub>3</sub> and prepared Ni-Cu/Al<sub>2</sub>O<sub>3</sub> catalysts for hydrogen production from methane and methanol fuels. *Int. J. Hydrol. Energy* **2013**, *38*, 1664–1675. [[CrossRef](#)]
28. Mrad, M.; Hammoud, D.; Gennequin, C.; Aboukais, A.; Abi-Aad, E. A comparative study on the effect of Zn addition to Cu/Ce and Cu/Ce-Al catalysts in the steam reforming of methanol. *Appl. Catal. A Gen.* **2014**, *471*, 84–90. [[CrossRef](#)]
29. Khzouz, M.; Gkanas, E.I.; Du, S.F.; Wood, J. Catalytic performance of Ni-Cu/Al<sub>2</sub>O<sub>3</sub> for effective syngas production by methanol steam reforming. *Fuel* **2018**, *232*, 672–683. [[CrossRef](#)]
30. Zhao, X.X.; Lu, G.X. Modulating and controlling active species dispersion over Ni-Co bimetallic catalysts for enhancement of hydrogen production of ethanol steam reforming. *Int. J. Hydrol. Energy* **2016**, *41*, 3349–3362. [[CrossRef](#)]
31. Ardiyanti, A.R.; Khromova, S.A.; Venderbosch, R.H.; Yakovlev, V.A.; Heeres, H.J. Catalytic hydrotreatment of fast-pyrolysis oil using non-sulfided bimetallic Ni-Cu catalysts on a delta-Al<sub>2</sub>O<sub>3</sub> support. *Appl. Catal. B Environ.* **2012**, *117*, 105–117. [[CrossRef](#)]
32. Leng, S.; Wang, X.; He, X.; Liu, L.; Liu, Y.E.; Zhong, X.; Zhuang, G.; Wang, J.G. NiFe/gamma-Al<sub>2</sub>O<sub>3</sub>: A universal catalyst for the hydrodeoxygenation of bio-oil and its model compounds. *Catal. Commun.* **2013**, *41*, 34–37. [[CrossRef](#)]
33. Nie, L.; de Souza, P.M.; Noronha, F.B.; An, W.; Sooknoi, T.; Resasco, D.E. Selective conversion of m-cresol to toluene over bimetallic Ni-Fe catalysts. *J. Mol. Catal. A Chem.* **2014**, *388*, 47–55. [[CrossRef](#)]
34. Han, Q.; Rehman, M.U.; Wang, J.; Rykov, A.; Gutiérrez, O.Y.; Zhao, Y.; Wang, X.; Ma, X.; Lercher, J.A. The synergistic effect between Ni sites and Ni-Fe alloy sites on hydrodeoxygenation of lignin-derived phenols. *Appl. Catal. B Environ.* **2019**, *253*, 348–358. [[CrossRef](#)]
35. Huynh, T.; Armbruster, U.; Kreyenschulte, C.; Nguyen, L.; Phan, B.; Nguyen, D.; Martin, A. Understanding the Performance and Stability of Supported Ni-Co-Based Catalysts in Phenol HDO. *Catalysts* **2016**, *6*, 176. [[CrossRef](#)]

36. Zhang, Z.; Pei, Z.; Chen, H.; Chen, K.; Hou, Z.; Lu, X.; Ouyang, P.; Fu, J. Catalytic in-Situ Hydrogenation of Furfural over Bimetallic Cu-Ni Alloy Catalysts in Isopropanol. *Ind. Eng. Chem. Res.* **2018**, *57*, 4225–4230. [CrossRef]
37. Moraes, M.S.A.; Migliorini, M.V.; Damasceno, F.C.; Georges, F.; Almeida, S.; Zini, C.A.; Jacques, R.A.; Caramão, E.B. Qualitative analysis of bio oils of agricultural residues obtained through pyrolysis using comprehensive two dimensional gas chromatography with time-of-flight mass spectrometric detector. *J. Anal. Appl. Pyrol.* **2012**, *98*, 51–64. [CrossRef]
38. Takanabe, K.; Nagaoka, K.; Nariai, K.; Aika, K.I. Titania-supported cobalt and nickel bimetallic catalysts for carbon dioxide reforming of methane. *J. Catal.* **2005**, *232*, 268–275. [CrossRef]
39. Singh, S.; Srivastava, P.; Singh, G. Synthesis, characterization of Co-Ni-Cu trimetallic alloy nanocrystals and their catalytic properties, Part-91. *J. Alloy Compd.* **2013**, *562*, 150–155. [CrossRef]
40. Ao, M.; Pham, G.H.; Sage, V.; Pareek, V.; Liu, S.M. Perovskite-derived trimetallic Co-Ni-Cu catalyst for higher alcohol synthesis from syngas. *Fuel Process. Technol.* **2019**, *193*, 141–148. [CrossRef]
41. Lua, A.C.; Wang, H.Y. Hydrogen production by catalytic decomposition of methane over Ni-Cu-Co alloy particles. *Appl. Catal. B Environ.* **2014**, *156*, 84–93. [CrossRef]
42. Shi, T.B.; Li, H.; Yao, L.H.; Ji, W.J.; Au, C.T. Ni-Co-Cu supported on pseudoboehmite-derived  $\text{Al}_2\text{O}_3$ : Highly efficient catalysts for the hydrogenation of organic functional groups. *Appl. Catal. A Gen.* **2012**, *425*, 68–73. [CrossRef]
43. Miranda, B.C.; Chimentao, R.J.; Szanyi, J.; Braga, A.H.; Santos, J.B.; Gispert-Guirado, F.; Llorca, J.; Medina, F. Influence of copper on nickel-based catalysts in the conversion of glycerol. *Appl. Catal. B Environ.* **2015**, *166*, 166–180. [CrossRef]
44. Chen, L.; Zhu, Q.S.; Wu, R.F. Effect of Co-Ni ratio on the activity and stability of Co-Ni bimetallic aerogel catalyst for methane Oxy- $\text{CO}_2$  reforming. *Int. J. Hydrot. Energy* **2011**, *36*, 2128–2136. [CrossRef]
45. Choi, H.Y.; Lee, W.Y. Effect of second metals and Cu content on catalyst performance of Ni-Cu/ $\text{SiO}_2$  in the hydrodechlorination of 1,1,2-trichloroethane into vinyl chloride monomer. *J. Mol. Catal. A Chem.* **2001**, *174*, 193–204. [CrossRef]
46. Chen, T.; Sun, Y.; Guo, M.; Zhang, M. Hydrothermal synthesis of Ni-Co-Cu alloy nanoparticles from low nickel matte. *J. Alloy Compd.* **2018**, *766*, 229–240. [CrossRef]
47. Mortensen, P.M.; Grunwaldt, J.D.; Jensen, P.A.; Jensen, A.D. Screening of Catalysts for Hydrodeoxygenation of Phenol as a Model Compound for Bio-oil. *Acs Catal.* **2013**, *3*, 1774–1785. [CrossRef]
48. Zhao, C.; Kasakov, S.; He, J.Y.; Lercher, J.A. Comparison of kinetics, activity and stability of Ni/HZSM-5 and Ni/ $\text{Al}_2\text{O}_3$ -HZSM-5 for phenol hydrodeoxygenation. *J. Catal.* **2012**, *296*, 12–23. [CrossRef]
49. Mortensen, P.M.; Grunwaldt, J.D.; Jensen, P.A.; Jensen, A.D. Influence on nickel particle size on the hydrodeoxygenation of phenol over Ni/ $\text{SiO}_2$ . *Catal. Today* **2016**, *259*, 277–284. [CrossRef]



© 2019 by the authors. Licensee MDPI, Basel, Switzerland. This article is an open access article distributed under the terms and conditions of the Creative Commons Attribution (CC BY) license (<http://creativecommons.org/licenses/by/4.0/>).